4D PET: Beyond Conventional Dynamic PET Imaging

Review Article

Arman Rahmim PhD, Jing Tang PhD

Department of Radiology, School of Medicine
Johns Hopkins University, Baltimore MD, USA

(Received 23 July 2008, Revised 15 August 2008, Accepted 25 August 2008)

ABSTRACT

In this paper, we review novel techniques in the emerging field of spatiotemporal 4D PET imaging. We will discuss existing limitations in conventional dynamic PET imaging which involves independent reconstruction of dynamic PET datasets. Various approaches that seek to attempt some or all of these limitations are reviewed in this work, including techniques that utilize iterative temporal smoothing, advanced temporal basis functions, principal components transformation of the dynamic data, wavelet-based techniques as well as direct kinetic parameter estimation methods. Extension of 4D PET to 5D PET in which the additional dimension of (respiratory or cardiac) gating is considered has also been discussed.

Key Words: PET, Spatiotemporal, 4D, Dynamic Imaging, 5D

Iran J Nucl Med 2008; 16(1): 1-13

Corresponding author: Arman Rahmim, PhD, Division of Nuclear Medicine, Department of Radiology, Johns Hopkins University School of Medicine, Baltimore MD 21287, USA
E-mail:arahmim1@jhmi.edu

1. INTRODUCTION AND MOTIVATION

One of the important aspects of nuclear medicine imaging using the PET modality is the inherent ability to perform dynamic imaging (*1*). This is a very notable capability allowing measurements of change in the bio-distribution of radiopharmaceuticals within the organ(s) of interest over time. This in turn offers very useful information about the underlying physiological or metabolic processes, as commonly extracted using various kinetic modeling techniques. Below we outline the three standard steps commonly performed in dynamic PET imaging:

Dynamic PET Acquisition

Dynamic PET acquisition can be performed using two general approaches depending on whether the scanner has the list-mode acquisition capability; i.e. the ability to store time-of-detection along with the spatial coordinates for the detected events (*2*). If such ability does not exist, the standard approach is to pre-specify, prior to data acquisition, the framing sequence of interest, and to bin the detected events in the corresponding sinograms to each frame. By contrast, the list-mode acquisition capability allows the added

flexibility of specifying the framing sequence post-acquisition. It is worth emphasizing that list-mode acquisition is distinct from list-mode reconstruction; the former (increasingly employed in PET scanners) is only a pre-requisite for the latter which offers added benefits in the image reconstruction task itself (*2*), as also mentioned in this paper in the context of 4D PET image reconstruction.

1.1 Dynamic PET Reconstruction

Following dynamic framing of the acquired data as outlined above, the common approach to dynamic PET imaging reconstruction consists of independently reconstructing tomographic data within each dynamic frame. Following this step, one arrives at a set of dynamic images intended to specify the variation of activity over time throughout the reconstructed field-of-view.

1.2 Dynamic Kinetic Parameter Estimation

Following the reconstruction step, the underlying functional parameters of interest (e.g. binding potential *BP*, maximum binding potential *Bmax*, dissociation constant of binding *Kd*, etc.) can be obtained using a number of tracer kinetic modeling techniques (e.g. see (*3*) for a review). Most commonly, compartmental modeling techniques are utilized, and are applied to time-activity-curves (TACs) extracted for either (i) particular regions of interest (ROIs), or (ii) at the voxel level, the latter resulting in *parametric images*.

1.3 Issues with Conventional Dynamic Imaging

The aforementioned standard approach to dynamic PET imaging suffers from three issues:
(1) The independent reconstruction of each of the (typically) many frames of the data can result in very noisy images.
(2) Conventional reconstruction assumes that the activity within each dynamic frame is static, thus resulting in potentially biased images.

To minimize the resulting bias from this assumption, one may instead use a higher number of frames to better sample activity variations over time; however, this will result in even higher noise levels (i.e. better addressing the second issue (bias) amplifies the first issue with noise; the inverse is also the case).
(3) Accurate application of tracer kinetic modeling requires knowledge and modeling of the noise distribution present in the reconstructed dynamic images (how noisy individual voxels are and how they correlate with other voxels), which can be extremely difficult and time-consuming to perform (*4, 5*). As a result, very commonly, presence of space-variant noise variance and inter-voxel correlations are simply ignored in kinetic parameter estimation.

In this review, we refer to the field encompassing techniques that attempt to address one or more of the aforementioned three issues as spatiotemporal 4D PET imaging. A wide range of methods have been proposed in the literature to this end, but they all agree in that they do *not* independently reconstruct individual dynamic frames, and these methods aim to outperform conventional dynamic PET (e.g. in terms of precision (noise) vs. accuracy (bias) trade-offs).

Relation with motion-compensation techniques: Here, we wish to note that while dynamic imaging and motion-compensated imaging methods overlap in a number of areas (since they both deal with varying activity distributions over time), yet the underlying bases of the two are different and need to be distinguished from one another; as such, this review deals with the former, while techniques to model and incorporate the latter have been reviewed by Rahmim *et al.* in (*6*).

In this review, we have broadly classified and elaborated 4D PET imaging techniques as those that utilize temporal smoothing (Sec. 2), advanced temporal basis functions (Sec. 3), principal components transformation of the dynamic data (Sec. 4), wavelet-based techniques (Sec. 5) and direct kinetic parameter estimation methods (Sec. 6). Furthermore, in Sec. 7, we have discussed an extension of this area to 5D PET imaging, involving dynamic, gated PET imaging.

2. ITERATIVE TEMPORAL SMOOTHING

2.1 A Common Approach

A common approach in this direction has been to impose temporal voxel smoothing within the reconstruction task.
This has been implemented via:
(i) Inter-iteration temporal smoothing (*7*) in which high-frequency noise-filtering is performed after every iteration of the reconstruction algorithm, with the assumption of similarity between nearby frames.
(ii) Maximum a posteriori probability (MAP) image reconstruction: in the standard framework, MAP-based methods[1] seek to minimize variations between spatial neighboring voxels. This approach can be

[1] This is also referred to as the Bayesian method (originally derived from a simple application of Bayes' rule to image reconstruction). It is also, sometimes, referred to as penalized likelihood (PL) image reconstruction.

extended to a 4D-MAP algorithm (e.g. see (*8*)) in which one uses a summation of spatial and temporal potential functions, in order to encourage smoothing between neighboring voxels in both the spatial and temporal directions.

Application of these approaches to dynamic PET (or SPECT) imaging has been shown to improve the noise performance of the reconstruction algorithms; nevertheless, they are *ad hoc* in that they assumes *a priori* that voxels in neighboring temporal frames have close values, and as such are bound to perform poorly for frames with fast dynamics. It must be noted that application of such methods in the context of motion-compensation, as reviewed in (*6*), is better conditioned since one can incorporate the extracted motion information within the 4D smoothing task (*9-11*), and not simply assume that each voxel has nearly constant values in nearby frames. In the rest of this paper, we describe techniques that attempt to more accurately model the underlying dynamic mechanism within the 4D image reconstruction task.

2.2 Model-Based Temporal Smoothing

Instead of encouraging temporally-adjacent voxels to have similar values, it makes more sense to encourage them to have intensity values along a kinetic fitted curve, as first investigated by Kadrmas and Gullberg (*12*) within the MAP framework. Thus, this approach effectively performs temporal smoothing of the intermediate images based on a parametric kinetic model. The extreme, special case of this method, investigated by Reader *et al.* (*13*), would simply *replace* the intermediate image estimates by the corresponding intensities found by fitting at each iteration. In general, while this overall approach is more sound that the previous one (Sec. 2.1), it is not known to be convergent, and in fact, suffers from the potentially problem that a specific kinetic model applied to intermediate image intensities that have not yet converged does not necessarily perform well, and thus does not necessarily result in improved algorithmic performance.

3. USE OF SMOOTH TEMPORAL BASIS FUNCTIONS

As mentioned in Sec. 1.3, conventional dynamic PET imaging methods specify framing sequences within which the data are independently reconstructed. This can be thought of as using the simplest possible temporal basis function, namely the rectangular-pulse, in the reconstruction task such that the data acquired in a particular frame do not contribute at all to other temporal frames.

An alternative approach would then aim at using other, smooth temporal basis functions in order to improve the quality of images by better relating data measured in different (especially adjacent) frames. Let us consider *N* temporal basis functions where $B_k(t)$ is used to denote the *k*th basis function (*k=1…N).* Then, the dynamic image set can be represented as:

$$\lambda_j(t) = \sum_{k=1}^{N} w_{jk} B_k(t) \qquad (1)$$

where $\lambda_j(t)$ represents the image intensity at location *j* at time *t,* and w_{jk} is the coefficient of the *k*th basis function at location *j*. In this context, the reconstruction task becomes to estimate the coefficients of the basis functions.

Various related approaches have been studies in the literature, which we classify below in terms of how the basis functions are defined; these include (i) model-driven, (ii) interpolating and (iii) data-driven definitions of basis functions, as we discuss next.

3.1 Model-Driven Basis Functions

It makes sense to consider basis functions extended temporally in accordance with some dynamic models describing how activities vary over time:

3.1.1 *Spectral analysis:* Meikle *et al.* (*14*) used the approach in which the basis functions were modeled as exponential functions of varying widths convolved with the arterial input function *q(t)* as initially proposed in (*15*):

$$B_k(t) = q(t) \otimes \exp(-\beta_k t) \qquad (2)$$

In this technique, the β values were fixed and chosen to cover the spectrum of expected kinetic behavior (for the particular biological imaging task). The authors then used the expectation-maximization (EM) technique to estimate the *w* coefficients (Eq. 1) of the basis functions from the data. This overall approach is somewhat specific to the imaging task of interest (range of β values need to be determined in advance); however, it can be applied to a wide range of tracer studies since it does not assume a specific compartmental model.

3.1.2 *Model-based principal components as basis functions:* In the context of the gamma camera (no reconstruction involved), Nijran and Barber (*16*)

proposed to generate a large range of theoretical curves from a particular tracer kinetic model, and then use principal components analysis (PCA) as applied to the covariance matrix between the generated curves to generate the most significant principal components, best representative of the data. This is because PCA is designed to generate vectors with maximized variations between them, such that only a small number of these principal components suffice for an adequate description of time-variations at any voxel. An extension of this approach, not explored in the literature to our knowledge, would be to use the generated principal components as temporal basis functions in the reconstruction tasks as applied to dynamic PET data. However, we emphasize again that the outlined approach would require advanced knowledge of the tracer kinetic model prior to the reconstruction tasks. Model-independent use of PCA is discussed in Sec. 4

3.2 Interpolating Basis Functions

In cases where the particular kinetic model is not known in advance, or is not accurately characterized, it is very desirable to consider temporal basis functions that are model-independent. Interpolating basis functions fit this criterion. The original motivation for their increasing use (*17-20*) in the reconstruction tasks can be seen by the following simple observation: the assumption that activity is constant within each dynamic frame, as used in conventional reconstruction techniques (see Sec. 1.3), is essentially equivalent to performing nearest-neighbor interpolation when considering a detected event; i.e. using a very simple rectangular pulse temporal basis function so that each event only contributes to the dynamic frame in which its detected.

Alternatively, one may consider utilizing interpolating basis functions to better sample the temporal variation of activity in each voxel. In fact, such an approach is commonly employed in the spatial domain: (i) in image representation, where relatively smooth basis functions are used to more accurately represent spatial activity distribution compared to using voxels (e.g. see (*21*)), and (ii) in forward/back-projection operations where more advanced interpolation techniques are utilized to improve images obtained compared to merely using nearest-neighbor interpolations.

A similar logic applies to the temporal domain: it makes very good sense to consider more sophisticated temporal basis functions so as to move beyond the commonly used nearest-neighbor temporal interpolation scheme.

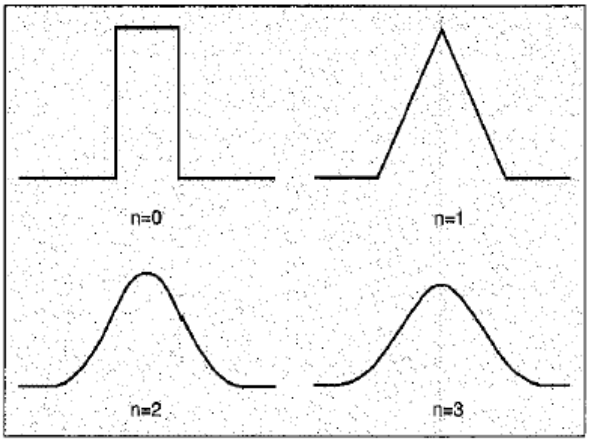

Fig. 1: B-spline basis functions of increasing orders (image courtesy of (*22*)).

In this regard, of very considerable potential and use have been the B-spline basis functions (*22-24*). These functions are very easily obtained by convolutions of the rectangular pulse function, as depicted in Fig. 1. Thus the 0^{th} order B-spline function is the rectangular function itself, corresponding to the nearest-neighbor interpolation, while the 1^{st} order function is the triangular function that is used for linear interpolation, and increasing orders correspond to higher degrees of interpolation.

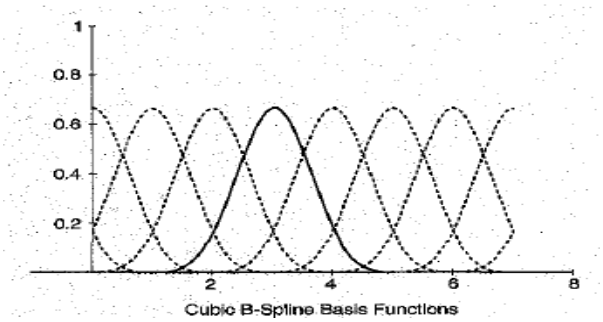

Fig. 2: Sampling a spatial or temporal domain via the cubic B-spline basis function (image courtesy of (*22*)).

B-spline basis function has been shown to have very favorable properties including being compact (thus efficient to implement) while minimizing errors (i.e. they fast approach the ideal interpolating function with few increasing orders). In fact, nowadays it is the 3^{rd} order cubic B-spline function that is most commonly

used to sample the spatial or temporal domain (Fig. 2) as it has very favorable efficiency/accuracy properties. This is in contrast with the ideal sinc function interpolator which is exact but does not have finite support and thus cannot be sampled efficiently.

In this context, a number of different reconstruction algorithms that aim to estimate the *w* coefficients in Eq. 1 have been proposed by a number of researchers, applied to histogrammed or list-mode data (*18-20*), and have been shown to result in kinetic parameter estimates with improved precision vs. accuracy trade-offs. Furthermore, these reconstruction algorithms were designed and shown to be convergent.

It is also worth noting that compared to histogram-mode reconstruction, intuitively it makes better sense to directly utilize list-mode data in the reconstruction task. This is because it can be presumed that compared to events measured at the beginning of a frame *m*, the data measured towards the end of that particular frame contain more information about the basis function coefficient for the next frame (*m*+1), and that by performing histogramming, this additional information is lost. By contrast, direct list-mode reconstruction maintains this information in the reconstruction task. In any case, this presumed advantage remains to be demonstrated in practice.

Furthermore, it must be noted that in the aforementioned works, the authors considered the use of *non-uniform* basis functions since early changes in concentration are typically much greater than those later in the study, and thus it makes sense to sample the temporal domain non-uniformly. Robust optimization of this non-uniform sampling remains to be fully studied, especially using analytic methods.

3.3 Data-Driven Temporal Basis Functions

In the aforementioned general approach, the *shapes* of the temporal basis functions are determined *a priori* independent of the particular study (though the non-sampling scheme, if performed at all, is often dependent on the study). An alternative is to instead use methods that determine the shapes of the basis functions adaptively in a data-driven sense. Below we describe two such approaches in the literature:

3.3.1 *Singular value decomposition (SVD):* Matthews *et al.* (*25*) used SVD as applied to dynamic PET images initially obtained using conventional reconstruction, in order to arrive at a set of useful temporal basis functions to be used in subsequent 4D image reconstruction (the EM formalism was used in this work to estimate the *w* coefficients in Eq. 1). The SVD technique has the advantage that in practice many of the singular values are insignificant when compared with the other dominant singular values, thus requiring only a subset to be used in the estimation task. A complication with this technique is that the resulting basis functions may contain negative values. However, this technique does not assume a kinetic model at all, and bases its results on a set of dynamic images initially obtained via standard reconstruction.

3.3.2 *Inter-reconstruction estimation:* An alternative approach has been to perform 4D reconstruction whereby the temporal basis functions themselves are also estimated as part of the reconstruction process (*26*), with the potential advantage of avoiding any *a priori* selection of the temporal basis functions, and utilizing a data-driven approach to do so.

This was implemented using an approach in which one first fixes the temporal basis functions (treating them as known), and estimates the corresponding *w* coefficients (see Eq. 1), and then alternates to an estimation algorithm in which the *w* coefficients are held as fixed and known, while the distributions of the temporal basis functions (at various temporal sampling points) are determined. A simultaneous updating procedure, not requiring to pre-specify the number of iterations inside each of the above two steps before switching to the other, was also outlines in (*27*) nearly halving the computation times. However, this approach may have some stability issues.

Overall, the aforementioned general approach, though potentially very promising, has not been shown to be a convergent algorithm. Furthermore it remains to be studied whether the proposed data-driven determination of basis functions outperforms the previous reconstruction algorithms outlined in Sec. 3.2.

4. PRINCIPAL COMPONENTS TRANSFORMATION OF THE DYNAMIC DATA

An alternative approach consists of performing principal components analysis (PCA), or transformation, on the dynamic data along the temporal direction. This is also sometimes referred to as the Karhunen-Loève (KL) transform[2]. PCA has been a popular technique for many years in various

[2] The term KL, however, is best applied to cases when the true ensemble covariance (and not the estimated sample covariance as is done in PCA) is known. Thus, in the experimental task of PET imaging where the object distribution is not known *a priori*, it is best to use the term PCA.

fields, particularly in geosciences and remote sensing, used to decorrelate multispectral images as used in compression, denoising and deblurring.

In the context of dynamic imaging, the general idea is that application of PCA to a time-series of images allows their decomposition into a number of factor images which are uncorrelated (i.e. with maximized variations between them). Since in practice only few of the factor images are sufficient to adequately describe the underlying dynamics, removal of the negligible factors renders a natural noise reduction technique. Such a denoising approach has been applied to nuclear medicine dynamic imaging in the past (e.g. model-based approach of (*16*) as reviewed in Sec. 3.1.2, and model-independent work of Kao *et al.* (*28*)). It must be noted that in the context of TAC extraction and noise-reduction, factor analysis techniques other than PCA have also been explored; e.g. see the works by El-Fakhri *et al.* (*29*) and Su *et al.* (*30*) for brief reviews and some novel techniques.

In the context of 4D image reconstruction, Wernick *et al. (31)* have made the observation that dynamic image sets in their standard forms are correlated in the temporal direction, and thus require 4D reconstruction algorithms that model and incorporate such temporal correlations (various approaches to this were discussed in previous sections). By contrast, the authors have proposed to first transform the standard dynamic datasets using PCA, and have shown that, with some simplifying assumptions, the resulting dynamic data sets become nearly uncorrelated and thus can be reconstructed independently, resulting in fast yet accurate reconstructions. Such an approach to 4D image reconstruction remains to be further investigated and expanded upon in the literature.

We conclude this section by noting that even though the aforementioned approach is originally designed for imaging of motion-free objects, it has been shown to work very well in reconstructing cardiac image sequences as well (*32*), and this is hypothesized *(31)* to be the case because the principal components model is able to capture the motion information in the form of motion-induced temporal fluctuations of the signal.

5. WAVELET-BASED TECHNIQUES

Wavelets are powerful mathematical tools for analysis of finite, non-periodic, and/or non-stationary signals. Wavelet transforms (WT) differ from traditional Fourier transforms by their inherent ability of localizing information in the time-frequency domain. The wavelets are scaled and translated copies (known as "daughter wavelets") of a finite-length or fast-decaying oscillating waveform (known as the "mother wavelet"). As an example, the first known and also the simplest possible wavelet is the Haar wavelet with its mother wavelet function $\psi(t)$ described as

$$\psi(t)=\begin{cases}1 & 0\le t<1/2,\\ -1 & 1/2\le t<1,\\ 0 & \text{otherwise.}\end{cases}$$

Fig. 3 shows the mother wavelet of Haar wavelet with some of its daughter wavelets.

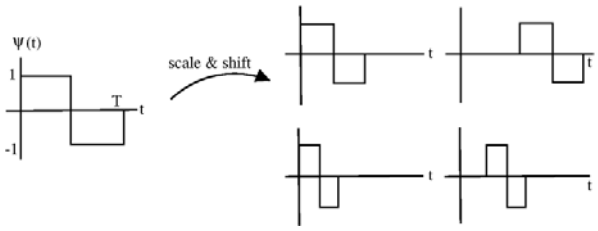

Fig. 3: Haar wavelet: Mother wavelet and some daughter wavelets.

Wavelets and multiscale methods have been widely applied in dynamic PET imaging, both for post-smoothing and in reconstruction. As we review next, in quantification analysis, multiscale denoising has been applied to reconstructed dynamic images at the voxel- or ROI-level. Wavelets have also been incorporated in emission tomographic reconstruction of individual image frames, and in spatiotemporal reconstruction of dynamic PET images.

5.1 Wavelet post-processing in dynamic PET

In the context of dynamic imaging, the one-dimensional wavelet transform has been applied in designing a time-varying filter to improve the signal-to-noise ratio in PET kinetic curves (*33*). A two-dimensional wavelet denoising algorithm was applied by Lin *et al.* (*34, 35*) to each short-axis image plane (of each individual image) independently in order to remove noise in the spatial domain, followed by application of one-dimensional wavelet denoising to the TAC for each ROI so as to also remove noise in the temporal domain.

Turkheimer *et al.* (*36, 37*) performed kinetic modeling in the wavelet domain. They applied the dyadic wavelet transform (DWT) to each dynamic frame to produce the correspondent wavelet transform. Kinetic modeling was then applied to wavelet coefficients of the time-curves. The wavelet coefficients were thresholded to reduce the level of noise and the remaining ones were subsequently

inverse wavelet transformed to produce the desired parametric images.

5.2 Wavelets in reconstruction tasks

Before their specific application in emission tomographic reconstruction, wavelets were incorporated in solving linear inverse problems, for example, with wavelet-vaguelette (*38*) and vaguelette-wavelet (*39*) decompositions followed by thresholding.

Kolaczyk (*40*) applied the aforementioned wavelet-vaguelette decomposition as well as wavelet shrinkage (WS) (*41*) in tomographic image reconstruction (single frame). A representation of the vaguelette coefficients corresponding to the Radon transform was developed. The representation led to an algorithm based on using the *analytic* FBP algorithm in a multi-resolution fashion to compute the vaguelette coefficients from the data. WS was applied as a method of regularization to the vaguelette coefficients before the inverse wavelet transform was performed to recover the image. A set of thresholds was used in WS, removing most of those coefficients corresponding to noise, while retaining most corresponding to the signal.

Multiscale analysis and regularization was also applied in *statistical* restoration and reconstruction (*42-45*). Nowak and Kolaczyk (*44*) developed a statistical multiscale framework for Poisson distributed data. The foundation of their Bayesian reconstruction framework was the multiscale factorization of the Poisson likelihood function. Conjugate priors were used in the multiscale parameter space in order to constrain how the intensity function was re-parameterized at each location-scale. The EM algorithm was applied in the MAP estimation problem, having a closed-form M-step. To avoid blockiness resulting from multi-resolution models formulated on a quadtree structure (a tree data structure in which each internal node has up to four children) (*44*), Frese *et al.* (*45*) proposed a wavelet graph prior model that exploited dependencies of wavelet coefficients across scales. The more general structure produces smoother estimates even for a Haar wavelet basis.

5.3 Wavelet in dynamic PET reconstruction

Although noticeable research has been performed in using tailored temporal basis functions for representing the time activity curves in dynamic PET reconstruction (see Sec. 3), Verhaeghe *et al.* (*46*) pioneered the research in using temporal wavelet basis functions. The L1-norm of the spatiotemporal wavelet coefficients of images served as the regularization term in the cost function to be minimized. Wavelets that were separable in space and time were utilized, with so-called B-spline wavelets in the spatial domain and E-spline wavelets in the temporal domain. The introduction of E-spline wavelets in the temporal domain was based on the concept that the activity distribution in the body is ruled by a system of differential equations involving compartmental models.

In a couple of dynamic PET simulations, one with a slice of the NCAT cardiac phantom and the other with a slice of the Zubal brain phantom, the regional signal-to-noise ratios (SNRs) from reconstructed noisy images were shown to be higher when temporal E-spline wavelets were applied compared to using temporal B-spline wavelets. The TACs extracted from a pixel in the left ventricle with wavelet regularization was shown to be closer to the true TAC. The spatiotemporal regularization reconstructed images were also shown to be less noisy than those with no regularization or with temporal regularization only (Fig. 4).

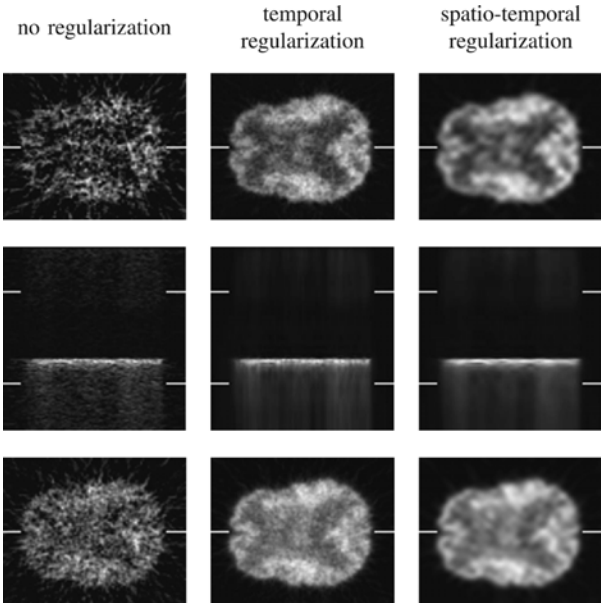

Fig. 4: Reconstructed brain phantom slices. Middle row are temporal slices. Time and space locations are indicated by the white bars. Upper and lower spatial slices correspond with the upper (early time) and lower (late time) bars in the temporal slice, respectively. Results in the third column give a good compromise between spatial and temporal regularization (images courtesy of (*46*)).

6. DIRECT KINETIC PARAMETER ESTIMATION

An alternative approach to conventional dynamic PET imaging has been to directly estimate kinetic parameters from the measured data, instead of generating reconstructed PET images from which the kinetic parameters are estimated, as depicted in Fig. 5.

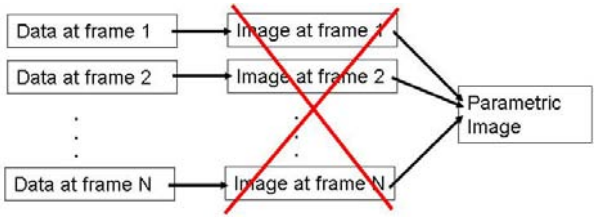

Fig. 5: Direct kinetic parameter estimation does not perform reconstruction of the individual frames, and instead estimates the parametric image collectively and directly from the data.

Broadly, there have been two general approaches in this context, the first one designed to improve speed and the second one to improve accuracy, as we describe next:

6.1 Generation of Parametric Sinograms

A technique explored in the past consisted of creating a 'parametric sinogram' from multiple dynamic sinograms by performing fitting (given a particular kinetic model) in the projection-space (and not the usual image-space); this was then followed by a *single* reconstruction. This approach has the benefit of reducing the computational burden by ~1 order of magnitude, and has been investigated for different parameter estimation tasks by a number of different authors (*47-50*). A limitation of this technique is that it is only applicable to models that can be expressed linearly in image-space such that they can be extended to the projection-space and thus be applied directly to the sinogram data. An additional issue is that while EM-type reconstruction algorithms assume that the data are Poisson-distributed, the data in the parametric sinograms may no longer be as such (e.g. this is the case when one extracts the Patlak slope from dynamic sinograms; slope of a fit to Poisson-distributed data is not Poisson-distributed itself).

6.2 Direct Parametric Estimation from Non-Combined Dynamic Data

With regards to the three limitations of conventional dynamic PET imaging outlined in Sec. 1.3, while many techniques discussed in this review attempt to address the first two by improving noise vs. bias performance, none address the third issue; i.e. the reconstructed images still contain very complex noise distributions that need to be modeled for accurate tracer kinetic modeling. Appropriate direct estimations of kinetic parameters from the dynamic data set can much simplify this task since such methods work directly with the measured data, which are very well known to follow the simple independent Poisson distribution. This approach was originally outlined in 1985 by Carson and Lange *(51)* in the very context of the EM algorithm. It sought to estimate kinetic parameters by maximizing the Poisson log-likelihood of obtaining the measured dynamic data.

However, this novel general outline was not actually implemented for a specific task at the time, and only in later years was this problem revisited by a number of different groups, as we review next. Just as there are two general categories of kinetic modeling techniques, namely ROI-based and voxel-based, we divide the direct estimation techniques in the literature into these two general categories:

6.2.1 ROI-based technique: A number of techniques have been proposed that aim to directly estimate the kinetic parameters at the ROI level from the PET (or SPECT) dynamic data. Vanzi *et al.* (*52*) investigated a method to extract renal kinetic parameters for a simple model with one uptake constant for each kidney. Huesman *et al. (53)* and Zeng *et al.* (*54*) developed methods to extract kinetic parameters in myocardial imaging using one-compartment and two-compartment methods, respectively[3].

The aforementioned methods first extracted the boundary information for the ROIs from standard reconstructions, followed by application of direct ROI parameter estimation form the data. Alternatively, Chiao *et al.* (*55*) developed techniques that *jointly* estimated, within a single reconstruction task applied to cardiac dynamic emission computed tomography (ECT), both the kinetic parameter estimates as well as the boundary information. An approach was also developed by the same authors (*56*) to use boundary side information (obtainable from high resolution MRI and CT images) within a similar direct reconstruction scheme.

[3] These two works were also designed to better address the existing problem in standard reconstructions for dynamic SPECT imaging, in which the rotation of the detectors while the distribution of the radiopharmaceutical changes over time result in inconsistent projections

6.2.2 Voxel-based technique: Kinetic parameter estimation at the voxel level (i.e. generation of parametric images) was achieved directly from dynamic PET data by Kamasak *et al. (57)*. The method was implemented for a specific compartmental model: the reversible two-tissue compartmental model with four kinetic parameters (k_1, k_2, k_3, k_4). Comparison of the method with standard techniques is shown in Fig. 6 for a simulated study, and exhibits clear improvements.

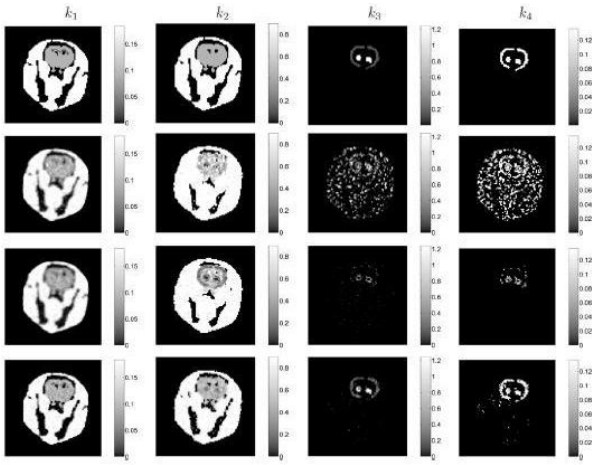

Fig. 6: Parametric images of k_1, k_2, k_3 and k_4 in (a) the original simulation, and reconstructed using standard dynamic reconstruction followed by (b) pixel-wise weighted least squares (PWLS) fitting, (c) PWLS with spatial regularization (PWLSR), and finally (d) the proposed direct parametric iterative coordinate descent (PICD) algorithm (images courtesy of *(57)*).

Majority of direct parametric reconstruction methods in the past have utilized nonlinear kinetic models to estimate individual kinetic parameters. On the other hand, a number of graphical modeling methods have been developed that yield simple linear/visual techniques for estimation/evaluation of kinetic properties of various PET tracers (e.g. see (*58*) for a review). The Patlak linear model for irreversible tracers was recently included in a direct parametric estimation task by Wang *et al.* (*59*), wherein the authors expanded the objective function for the reconstruction task to directly relate the Patlak parameters across the image to measured data, and used a preconditioned conjugate gradient algorithm to find the optimum solution.

Within a similar Patlak estimation task, Tang *et al.* (*60*) alternatively extended the system matrix formulation and derived a direct 4D EM parametric reconstruction algorithm, having had the advantages of being both accurate in its formulation and being a closed-form reconstruction algorithm.

In a later work, Wang and Qi (*61*) used the method of paraboloidal surrogate functions (*62*) (which approximates the Poisson log-likelihood function by local parabolas thus considerably simplifying the optimization task) to derive a very feasible direct estimation technique. The method was shown to effectively reduce to two steps at each iteration; defining $\hat{\lambda}_{jm}^{n+1}$ as the (n+1)th updated image value at voxel j and frame m, and $\lambda(\kappa_j^n)$ as the calculated image intensity given the present estimated kinetic parameters (summarized by the vector κ_j^n of kinetic parameters at voxel j), these two steps are:
(i) Image update step:

$$\hat{\lambda}_{jm}^{n+1} = \lambda(\kappa_j^n) + \frac{g_{jm}^n}{w_{jm}^n}$$

and (ii) kinetic fitting

$$\kappa_j^{n+1} = \arg\max_{\kappa_j} \left\{ -\sum w_{jm}^n \left(\lambda(\kappa_j) - \hat{\lambda}_{jm}^{n+1} \right)^2 \right\}$$

where g_{jm}^n denotes the gradient of the penalized log-likelihood at pixel j in frame m at the nth iteration, and w_{jm}^n is a weighting factor determined by the specific algorithm. The developed algorithm has the great advantage that it is fairly straight-forward to implement, and that the second part resembles the least-squares optimization task, as utilized by a wide variety of kinetic modeling tasks, except that the weights are now accurately determined and not chosen on an *ad hoc* basis.

It is worth noting that the major limitation of these techniques is that the kinetic model has to be known in advance prior to reconstruction and to apply well to all areas in the image, the latter not being exactly the case in many imaging scenarios, thus potentially necessitating approximation schemes.

We conclude this section by noting that the methods discussed in sections 3.1.1 and 3.1.2 can also be considered as direct estimation tasks, since the smooth temporal basis function were based on underlying biological models, and the extracted coefficients conveyed how much each biological factor contributed to the data. This was also the case for the SVD method discussed in 3.3.1 which was argued by the authors to

distinguish the separate biological contributions to the data. Nevertheless, since these methods all involved the use of smooth temporal basis functions, we discussed them in Sec. 3.

7. 5D PET IMAGING

The aforementioned techniques can also be used for the natural extension of 4D PET imaging to 5D PET imaging, by including an additional dimension coming from gating (cardiac or respiratory). In present applications, dynamic *and* gated imaging is rarely performed since standard independent reconstruction of the individual dynamic, gated PET data would result in considerably noisy images. However, this could be of interest in a number of areas. For instance, in dynamic-cardiac imaging, ^{13}N-labeled ammonia ($^{13}NH_3$) can be used for the measurement of myocardial blood flow which makes it possible to measure blood flow at the level of micro-circulation. Addition of cardiac gating to dynamic imaging has the advantage of reducing cardiac motion artifacts.

Verhaeghe *et al.* (*63*) have taken an important step in this direction by using B-spline temporal basis functions (see Sec. 3.2) to represent both the temporal and gate dimensions. As shown in Fig. 7, standard reconstructions result in noisy images, which upon post-smoothing result in loss of detail. By contrast, advanced 5D imaging using temporal basis functions results in improved noise performance while maintaining sharply defined images.

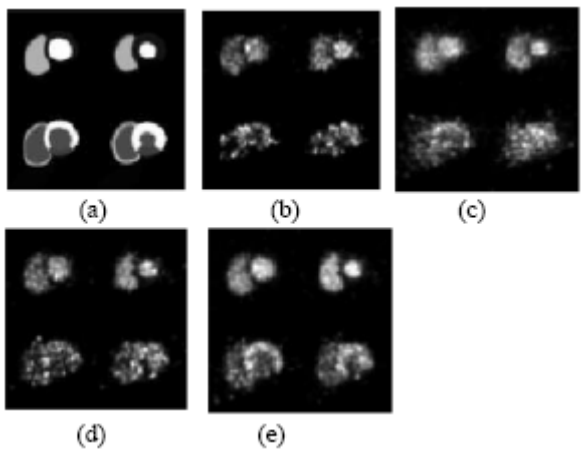

Fig. 7: (a) Short axis view of a simulated phantom, and the resulting images obtained via standard reconstruction (b) without and (c) with post-smoothing, and using (d) first-order and (e) third-order (i.e. cubic) B-spline temporal basis functions in the temporal and gate dimensions (images courtesy of (*63*)).

It must however be noted that, as mentioned in Sec. 1.3, dynamic imaging and motion-compensated imaging (e.g. in cardiac) involve different fundamentals. Therefore, even though a number of techniques discussed in this work have also been in the past used for motion compensated image reconstruction (e.g. temporal smoothing, use of temporal basis functions, PCA), motion-compensation is best treated distinctly and with more direct consideration of motion itself, as reviewed in (*6*).

8. CONCLUSION

The present work has attempted to summarize important themes in the emerging field of 4D PET imaging, the objective being to address existing issues with conventional dynamic PET imaging. The issues arising from independent reconstructions of acquired dynamic PET frames were summarized as the generation of noisy images, biased images (as the activity within a frame is conventionally assumed constant) and the considerable complexity of modeling the generated noise in the images in the kinetic modeling step.

A wide range of techniques designed to address some or all of these issues were discussed, including techniques that utilize iterative temporal smoothing, smooth temporal basis functions, principal components transformation of the dynamic data, wavelet-based techniques as well as direct kinetic parameter estimation methods.

Finally, it is worth emphasizing that while indirect methods still face the very difficult task of estimating noise correlations in reconstructed images for kinetic modeling purposes (often neglected for simplicity), the latter category which directly estimate kinetic parameters from the measured data are able to naturally address this difficulty since they accurately model the known uncorrelated Poisson noise distribution in the PET data.

9. REFERENCES

1. Rahmim A, Cheng J-C, Blinder S, Camborde M-L, Sossi V. Statistical dynamic image reconstruction in state-of-the-art high-resolution PET. Phys Med Biol. 2005;20: 4887-4912.

2. Rahmim A, Lenox M, Reader AJ, et al. Statistical list-mode image reconstruction for the high resolution research tomograph. Phys Med Biol. 2004;49(18):4239-4258.

3. Bentourkia M, Zaidi H. Tracer kinetic modeling in PET. PET Clinics. 2007;2(2):267-277.

4. Barrett H, Wilson D, Tsui B. Noise properties of the EM algorithm: I. Theory. Phys Med Biol. 1994;39(5):833-846.

5. Qi J. A unified noise analysis for iterative image estimation. Phys Med Biol. 2003;48:3505-3519.

6. Rahmim A, Rousset OG, Zaidi H. Strategies for motion tracking and correction in PET. PET Clinics. 2007;2(2):251-266.

7. Walledge RJ, Manavaki R, Honer M, Reader AJ. Inter-frame filtering for list-mode EM reconstruction in high-resolution 4-D PET. IEEE Trans Nucl Sci. 2004;51(3):705-711.

8. Taek-Soo L, Segars WP, Tsui BMW. Study of parameters characterizing space-time Gibbs priors for 4D MAP-RBI-EM in gated myocardial perfusion SPECT. Paper presented at: Nuclear Science Symposium Conference Record, 2005 IEEE, 2005.

9. Lalush DS, Lin C, Tsui BMW. A priori motion models for four-dimensional reconstruction in gated cardiac SPECT. Paper presented at: IEEE Nuclear Science Symposium Conference Record, 1996.

10. Gravier EJ, Yang Y. Motion-compensated reconstruction of tomographic image sequences. IEEE Trans Nucl Sci. 2005;52(1):51-56.

11. Gravier E, Yang Y, King MA, Jin M. Fully 4D motion-compensated reconstruction of cardiac SPECT images. Phys Med Biol. 2006;51(18):4603-4619.

12. Kadrmas DJ, Gullberg GT. 4D maximum a posteriori reconstruction in dynamic SPECT using a compartmental model-based prior. Phys Med Biol. 2001;46(5):1553-1574.

13. Reader AJ, Matthews JC, Sureau FC, Comtat C, Trebossen R, Buvat I. Iterative Kinetic Parameter Estimation within Fully 4D PET Image Reconstruction. Paper presented at: Nuclear Science Symposium Conference Record, 2006. IEEE, 2006.

14. Meikle SR, Matthews JC, Cunningham VJ, et al. Parametric image reconstruction using spectral analysis of PET projection data. Phys Med Biol. 1998;43(3):651-666.

15. Snyder DL. Parameter Estimation for Dynamic Studies in Emission-Tomography Systems Having List-Mode Data. IEEE Trans Nucl Sci. 1984;31(2):925-931.

16. Nijran KS, Barber DC. Towards automatic analysis of dynamic radionuclide studies using principal-components factor analysis. Phys Med Biol. 1985;30(12):1315-1325.

17. Zibulevsky M. ML reconstruction of dynamic PET images from projections and Clist. Paper presented at: Nuclear Science Symposium, 1999. Conference Record. 1999 IEEE, 1999.

18. Li Q, Asma E, Ahn S, Leahy RM. A fast fully 4-D incremental gradient reconstruction algorithm for list mode PET data. IEEE Trans Med Imaging. 2007;26(1):58-67.

19. Nichols TE, Qi J, Asma E, Leahy RM. Spatiotemporal reconstruction of list-mode PET data. IEEE Trans Med Imaging. 2002;21(4):396-404.

20. Verhaeghe J, D'Asseler Y, Vandenberghe S, Staelens S, Lemahieu I. An investigation of temporal regularization techniques for dynamic PET reconstructions using temporal splines. Med Phys. 2007;34(5):1766-1778.

21. Matej S, Lewitt RM. Practical considerations for 3-D image reconstruction using spherically symmetric volume elements. IEEE Trans Med Imaging. 1996;15(1):68-78.

22. Unser M, . Splines: a perfect fit for signal and image processing. IEEE Signal Process Mag. 1999;16:22-38.

23. Unser M. Sampling-50 years after Shannon. Proceedings of the IEEE. 2000;88(4):569-587.

24. Thevenaz P, Blu T, Unser M. Interpolation revisited [medical images application]. IEEE Trans Med Imaging. 2000;19(7):739-758.

25. Matthews J, Bailey D, Price P, Cunningham V. The direct calculation of parametric images from dynamic PET data using maximum-likelihood iterative reconstruction. Phys Med Biol. Jun 1997;42(6):1155-1173.

26. Reader AJ, Sureau FC, Comtat C, Trebossen R, Buvat I. Joint estimation of dynamic PET images and temporal basis functions using fully 4D ML-EM. Phys Med Biol. 2006;51(21):5455-5474.

27. Reader AJ, Sureau F, Comtat C, Trebossen R, Buvat I. Simultaneous Estimation of Temporal Basis Functions and Fully 4D PET Images. Paper presented at: Nuclear Science Symposium Conference Record, 2006. IEEE, 2006.

28. Chien-Min K, Yap JT, Mukherjee J, Wernick MN. Image reconstruction for dynamic PET based on low-order approximation and restoration of the sinogram. IEEE Trans Med Imaging. 1997;16(6):738-749.

29. El Fakhri G, Sitek A, Guerin B, Kijewski MF, Di Carli MF, Moore SC. Quantitative dynamic cardiac 82Rb PET using generalized factor and compartment analyses. J Nucl Med. 2005;46(8):1264-1271.

30. Su Y, Welch MJ, Shoghi KI. The application of maximum likelihood factor analysis (MLFA) with

uniqueness constraints on dynamic cardiac microPET data. Phys Med Biol. 2007;52(8):2313-2334.

31. Wernick MN, Infusino EJ, Milosevic M. Fast spatio-temporal image reconstruction for dynamic PET. IEEE Trans Med Imaging. 1999;18(3):185-195.

32. Narayanan MV, King MA, Soares EJ, Byrne CL, Pretorius PH, Wernick MN. Application of the Karhunen-Loeve transform to 4D reconstruction of cardiac gated SPECT images. IEEE Trans Nucl Sci. 1999;46(4):1001-1008.

33. Millet P, Ibanez V, Delforge J, Pappata S, Guimon J. Wavelet analysis of dynamic PET data: Application to the parametric imaging of benzodiazepine receptor concentration. Neuroimage. 2000;11(5):458-472.

34. Lin JW, Laine AF, Bergmann SR. Improving PET-based physiological quantification through methods of wavelet denoising. IEEE Trans Biomed Eng. 2001;48(2):202-212.

35. Lin JW, Laine AF, Akinboboye O, Bergmann SR. Use of wavelet transforms in analysis of time-activity data from cardiac PET. J Nucl Med. 2001;42(2):194-200.

36. Turkheimer FE, Banati RB, Visvikis D, Aston JAD, Gunn RN, Cunningham VJ. Modeling dynamic PET-SPECT studies in the wavelet domain. J Cereb Blood Flow Metab. 2000;20(5):879-893.

37. Turkheimer FE, Aston JAD, Banati RB, Riddell C, Cunningham VJ. A linear wavelet filter for parametric imaging with dynamic PET. IEEE Trans Med Imaging. 2003;22(3):289-301.

38. Donoho DL, Johnstone IM, Kerkyacharian G, Picard D. Wavelet Shrinkage - Asymptopia. J Roy Stat Soc B. 1995;57(2):301-337.

39. Abramovich F, Silverman BW. Wavelet decomposition approaches to statistical inverse problems. Biometrika. 1998;85(1):115-129.

40. Kolaczyk ED. A wavelet shrinkage approach to tomographic image reconstruction. J Am Stat Assoc. 1996;91(435):1079-1090.

41. Donoho DL, Johnstone IM. Ideal Spatial Adaptation by Wavelet Shrinkage. Biometrika. 1994;81(3):425-455.

42. Figueiredo MAT, Nowak RD. An EM algorithm for wavelet-based image restoration. IEEE Trans Med Imaging. 2003;12(8):906-916.

43. Bhatia M, Karl WC, Willsky AS. A wavelet-based method for multiscale tomographic reconstruction. IEEE Trans Med Imaging. 1996;15(1):92-101.

44. Nowak RD, Kolaczyk ED. A statistical multiscale framework for Poisson inverse problems. IEEE Trans Inform Theory. 2000;46(5):1811-1825.

45. Frese T, Bouman CA, Sauer K. Adaptive wavelet graph model for Bayesian tomographic reconstruction. IEEE Trans Image Process. 2002;11(7):756-770.

46. Verhaeghe J, Van De Ville D, I. K, D'Asseler Y, Lemahieu I, Unser M. Dynamic PET reconstruction using wavelet regularization with adapted basis functions. IEEE Trans Med Imaging. 2008;27(7):943-959.

47. Tsui E, Budinger TF. Transverse section imaging of mean clearance time. Phys Med Biol. 1978;23(4):644-653.

48. Huang SC, Carson RE, Phelps ME. Measurement of local blood flow and distribution volume with short-lived isotopes: a general input technique. J Cereb Blood Flow Metab. 1982;2(1):99-108.

49. Alpert NM, Eriksson L, Chang JY, et al. Strategy for the measurement of regional cerebral blood flow using short-lived tracers and emission tomography. J Cereb Blood Flow Metab. 1984;4(1):28-34.

50. Maguire RP, Calonder C, Leenders KL. Patlak analysis applied to sinogram data. In: R Myers VC, D Bailey and T Jones, ed. Quantification of Brain Function Using PET. San Diego: Academic; 1996:307-311.

51. Carson RE, Lange K. The EM parametric image reconstruction algorithm. J Am Statist Assoc. 1985;80:20-22.

52. Vanzi E, Formiconi AR, Bindi D, LaCava G, Pupi A. Kinetic parameter estimation from renal measurements with a three-headed SPECT system: a simulation study. IEEE Trans Med Imaging. 2004;23(3):363-373.

53. Huesman RH, Reutter BW, Zeng GL, Gullberg GT. Kinetic parameter estimation from SPECT cone-beam projection measurements. Phys Med Biol. 1998;43(4):973-982.

54. Zeng GL, Gullberg GT, Huesman RH. Using linear time-invariant system theory to estimate kinetic parameters directly from projection measurements. IEEE Trans Nucl Sci. 1995;42(6):2339-2346.

55. Ping-Chun C, Rogers WL, Clinthorne NH, Fessler JA, Hero AO. Model-based estimation for dynamic cardiac studies using ECT. IEEE Trans Med Imaging. 1994;13(2):217-226.

56. Ping-Chun C, Rogers WL, Fessler JA, Clinthorne NH, Hero AO. Model-based estimation with boundary side

information or boundary regularization [cardiac emission CT]. IEEE Trans Med Imaging. 1994;13(2):227-234.

57. Kamasak ME, Bouman CA, Morris ED, Sauer K. Direct reconstruction of kinetic parameter images from dynamic PET data. IEEE Trans Med Imaging. 2005;24(5):636-650.

58. Logan J. Graphical analysis of PET data applied to reversible and irreversible tracers. Nucl Med Biol. 2000;27(7):661-670.

59. Wang G, Fu L, Qi J. Maximum a posteriori reconstruction of the Patlak parametric image from sinograms in dynamic PET. Phys Med Biol. 2008;53(3):593-604.

60. Tang J, Kuwabara H, Wong DF, Rahmim A. Direct 4D reconstruction of parametric images incorporating anato-functional joint entropy. IEEE NSS/MIC Conf Proceed. 2008.

61. Wang G, Qi J. Iterative nonlinear least squares algorithms for direct reconstruction of parametric images from dynamic PET. Paper presented at: Biomedical Imaging: From Nano to Macro, 2008. ISBI 2008. 5th IEEE International Symposium on, 2008.

62. Fessler JA, Erdogan H. A paraboloidal surrogates algorithm for convergent penalized-likelihood emission image reconstruction. Paper presented at: Nuclear Science Symposium, 1998. Conference Record. 1998 IEEE, 1998.

63. Verhaeghe J, D'Asseler Y, Staelens S, Vandenberghe S, Lemahieu I. Reconstruction for gated dynamic cardiac PET imaging using a tensor product spline basis. IEEE Trans Nucl Sci. 2007;54(1):80-91.